

Investigate Curvature Angle of the Blade of Banki's Water Turbine Model for Improving Efficiency by Means Particle Swarm Optimization

Lie Jasa*[‡], I Putu Ardana**, Ardyono Priyadi***, Mauridhi Hery Purnomo****

*Department of Electrical Engineering, Udayana University, Denpasar, Bali, Indonesia

**Department of Electrical Engineering, Udayana University, Denpasar, Bali, Indonesia

***Department of Electrical Engineering, Sepuluh Nopember Institute of Technology, Surabaya, Indonesia

****Department of Electrical Engineering, Sepuluh Nopember Institute of Technology, Surabaya, Indonesia

(liejasa@unud.ac.id, ardana@unud.ac.id, priyadi@ee.its.ac.id, hery@ee.its.ac.id)

[‡]Corresponding Author; Lie Jasa, Department of Electrical Engineering, Kampus Unud Bukit Jimbaran Badung, Bali 80623, Indonesia, Tel: +62 0361 703315, Fax: +62 361 703315, liejasa@unud.ac.id

Received: 16.09.2016 Accepted:09.12.2016

Abstract-Turbines are used to convert potential energy into kinetic energy. Turbine blades are designed expertly with specific curvature angles. The output power, speed, and efficiency of a water turbine are affected by the curvature angle of the blade because water energy is absorbed by the blade in contact with the water flow. The particle swarm optimization (PSO) algorithm can be used to design and optimize micro hydro turbines. In this study, the blade curvature angle in a Banki's water turbine model is investigated using the particle swarm optimization algorithm to obtain the highest output power, speed, and efficiency in the water turbine. Mathematical and experimental models are employed to investigate the blade curvature angle. The result shows that a curvature angle of 15° provides higher output power, speed, and efficiency than angles of 16° and 17°, despite the fact that 16° is commonly used in commercial production.

Keywords blades, turbine, PSO, hydropower.

1. Introduction

Today, energy resources play an important role in economics, politics, social life, and the sciences. This is especially so in Indonesia where conventional energy resources are decreasing and prices are tending to rise [1]. Renewable energy [2] sources can potentially substitute for conventional energy resources and to smoothly solve these problems [3]. Indonesia has many renewable energy resources, including river water, sea water flow, tides, wind, and geothermal and solar energies, however hydropower plants are predominantly used for renewable energy supply as compared with the other alternatives [4], [5], [6]. One type of hydropower is micro-hydro power, which has become popular since it is simpler in its design, easier and cheaper to operate, faster to install, and has lower environmental impacts than the others [7].

The water turbine is a simple machine usually made of wood or steel with a fixed blade attached to a surrounding wheel [8], [9]. This blade is driven by a stream of water flowing around the wheel. Water pressure on the blade produces torque on the shaft to make the wheel spin [10]. The potential energy in the accumulated water continuously applied to the blade attached to the turbine wheel generates kinetic energy on the turbine shaft [11]. Sometimes the water flows vertically at the top, the middle, or the bottom of the turbine wheel. The curvature angle of the blade is a key issue in the energy conversion process.

One type of water turbine model is called the Banki's model. The theory behind the Banki's model, written by Mockmore and Merryfield in 1949, can be found in reference [12]. In the Banki's water turbine, the nozzle [12], whose cross-sectional area is rectangular, discharges a jet into the full width of the wheel, and is oriented at an angle of 16 degrees to the tangent of the wheel's periphery. More simply stated,

the curvature angle of the blade is 16 degrees. Based on reference[12], the authors argued that the curvature angle is the key for obtaining the highest possible output power, speed, and efficiency of the water turbine.

This study explores mathematical and experimental design models of the Banki's water turbine to investigate the performances resulting from 15°, 16°, and 17° blade curvature angles. Our goal is to determine the optimal turbine parameters for achieving the highest possible power output, efficiency, and speed. The mathematical models explored in our research are governed by principles of conservation of mass, momentum, and energy, and are described in detail in section 2. From the mathematical model we use, optimum parameter characteristics are simulated by the particle swarm optimization (PSO) [13], method to obtain the optimal blade curvature angle. Then, experimental design models are used to clarify the blade's curvature angle obtained by PSO to assess whether or not it yields maximum values for all of the parameters. In order to validate the performance of the each experimental turbine model, it was necessary to utilize the same turbine model parameters, including wheel diameter, thickness, material, number of blades, water discharge, and load generators.

2. The Banki Formula

2.1 Theoretical Background

The Banki's turbine, as described in[12], consists of a nozzle and a turbine runner. The runner is built of two parallel circular disks joined at their rims with a series of curved blades. The nozzle, whose cross-sectional area is rectangular, discharges a jet of water the full width of the wheel, which enters the wheel at an angle of 16 degrees to the tangent of the wheel's periphery. The shape of the jet is rectangular, wide, and fairly shallow. The water strikes the blades on the rim of the wheel, as shown in Figure 1, flows over the blade, then leaves it, passing through the empty space between the inner rims, enters a blade on the inner side of the rim, and is then discharged at the outer rim. The wheel is an inward jet wheel. Since the flow is essentially radial, the diameter of the wheel does not practically depend on the amount of water impact, and neither does the desired wheel breadth depend on the quantity of water.

The path of the jet through the turbine is assumed to be that at the centre of point A, as shown in Figure 1, at an angle of α_1 tangent to the periphery. So the velocity of the jet path water through the turbine can be written as follows:

$$V_1 = C\sqrt{2gH} \tag{1}$$

The relative velocity of the water at the entrance, v_1 , can be found at u_1 if the peripheral velocity of the wheel at that point is known. β_1 is the angle between the forward directions of the two latter velocities.

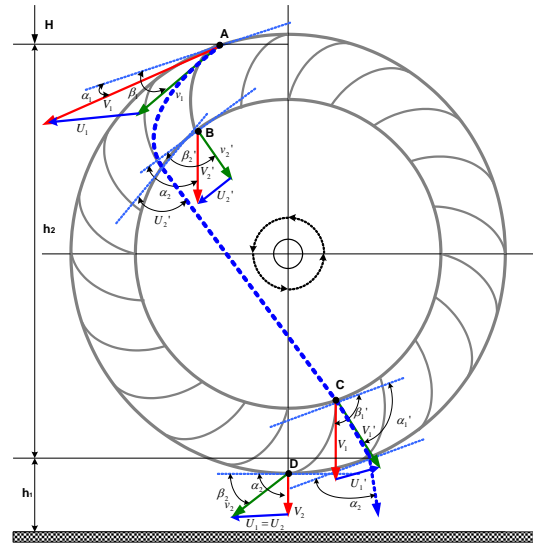


Fig.1. Path of water through turbine^[11]

For maximum efficiency, the angle of the blade should equal β_1 . Line AB represents the relative velocity of blade v_2' and β_2' represents the peripheral velocity of the wheel at that point. An absolute velocity of the water at the exit of blade v_2' can be determined by v_2' , β_2' , and v_2 . The angle between the absolute velocity and the velocity of the wheel at this point is α_2' . The absolute path of the water when it is flowing over blade AB can be determined, as can the actual point when it leaves the blade. An absolute velocity V_2' assumes a constant value, so that V_1' can be obtained at point C. This means the absolute velocity V_1' is equal to V_2' . Based on this statement, we can state that blade CD is equal to blade AB and $\alpha_1' = \alpha_2'$, $\beta_1' = \beta_2'$, $\beta_1 = \beta_2$.

The efficiency of the output power is given as

$$HP_{out} = \left(\frac{\omega Q u_1}{g}\right) (V_1 \cos \alpha_1 - u_1) (1 + \psi \cos \beta_2 / \cos \beta_1) \tag{2}$$

And the input power may be stated as $HP_{in} = \frac{\omega Q H}{g}$

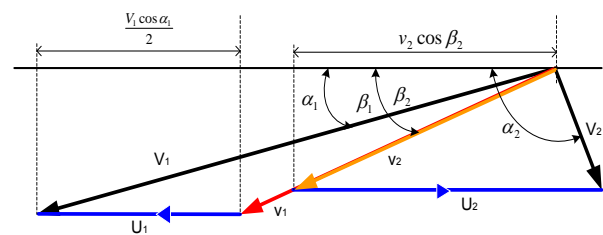


Fig. 2. Velocity diagram ^[11]

Based on Equation (1), we obtain $H = \frac{V_1^2}{C^2 2g}$ And substituting into Equation (3), we obtain $HP_{in} = \omega Q V_1^2 / C^2 2g$. Efficiency is defined by the ratio of the output and input power, $\eta = \frac{H_{out}}{H_{in}}$, $\eta = (2C^2 u_1 / V_1) (\cos \alpha_1 - u_1 / V_1) (1 + \psi \cos \beta_2 / \cos \beta_1)$, When $\beta_1 = \beta_2$,

$$\eta = (2C^2 u_1 / V_1) (1 + \psi) (\cos \alpha_1 - u_1 / V_1) \tag{3}$$

Assuming that Equation (3) is a function and u_1 / V_1 is an observing variable. The first differentiation of Equation (3) is

equal to zero, and is given by, $u_1/V_1 = \cos \alpha_1/2$, Maximum efficiency is given by $\eta_{max} = (\frac{1}{2}C^2) (1 + \psi) (\cos^2 \alpha_1)$ Based on Figure 2, the direction of V_2 is not radial when $u_1 = \frac{1}{2}V_1\alpha_1$. The water flow of the outer of rim should be radial. Therefore, the value of u_1 is given by

$$u_1 = \left[\frac{C}{(1+\psi)} \right] (V_1 \cos^2 \alpha_1) \tag{4}$$

When there are no losses on the head due to friction in the nozzle or the blades, ψ and C have unity values.

Variations in the nozzle roughness coefficient C is a quadratic function, as stated at Equation (4). There are two types of hydraulic losses from this nozzle aspect that occur when water is striking the outer and inner peripheries. These losses are relatively small when the blade thickness is sufficiently thin and should not exceed the jet so, as shown in Figure 3. Therefore, the water energy will strike the outer and inner peripheries of the blade. The blade system can provide the optimal blade roughness coefficient ψ , 0.98, when the number and thickness of the blades is accurately obtained.

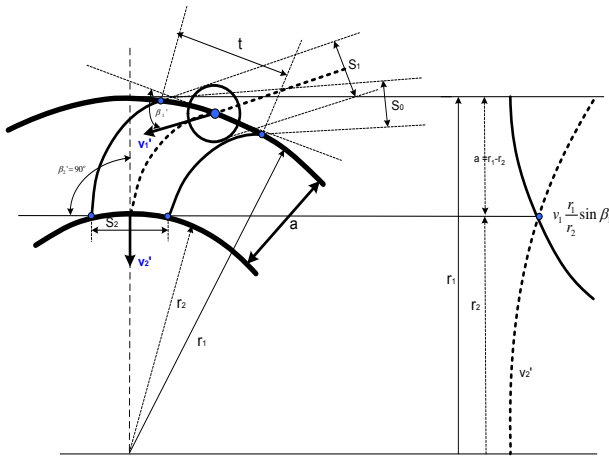


Fig. 3. Blade Spacing [11]

2.2 Design Construction Formula

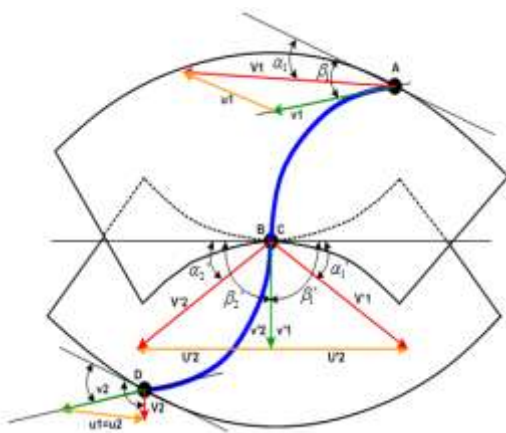


Fig. 4. Composite velocity diagram [11]

2.2.1 Blade Angle

As stated in Figures 1 and 3, the blade angle β_1 can be calculated by $u_1 = \frac{1}{2}V_1 \cos \alpha_1$ and $\tan \beta_1 = 2 \tan \alpha_1$. Based on Figures 4 and 5, the velocity of V_1' can be obtained as $V_1' = [2gh_2 + (V_2')^2]^{\frac{1}{2}}$

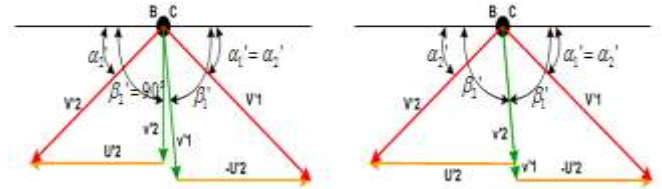


Fig. 5. Velocity Diagram [11]

2.2.2. Width of the Radial Rim

The thickness of the entrance jet s_1 for a distance of blade t can be calculated by

$$s_1 = t \sin \beta_1 \tag{5}$$

The inner exit blade spacing s_2 for $a = r_1 - r_2$ can be obtained by $s_2 = t(r_1/r_2)$ where $s_2 = v_1 s_1 / v_2'$ to find the value of β_1 requires a velocity v_2' influenced by the centrifugal force, and is given by

$$(v_1)^2 - (v_2')^2 = (u_1)^2 - (u_2')^2$$

$$(v_2') = v_1 \left(\frac{s_1}{s_2} \right) = v_1 \left(\frac{r_1}{r_2} \right) \sin \beta_1$$

$$x^2 - \left[1 - \left(\frac{v_1}{u_1} \right)^2 \right] x - \left(\frac{v_1}{u_1} \right)^2 \sin^2 \beta_1 = 0$$

$$\frac{v_1}{u_1} = \frac{1}{\cos \beta_1}$$

$$\text{where } x = (r_2 / r_1)^2$$

Based on Figure 6, the central angle BOC can be calculated by

$$(v_1)^2 - (v_2')^2 = (u_1)^2 - (u_2')^2$$

$$(v_2')^2 = v_1 \left(\frac{s_1}{s_2} \right) = v_1 \left(\frac{r_1}{r_2} \right) \sin \beta_1$$

$$\tan \alpha_2' = \frac{v_2'}{u_2}$$

$$\text{boC} = 2 \alpha_2' \tag{6}$$

2.2.3 Wheel diameter and axial wheel breadth

The wheel diameter can be determined from Equations. $u_1 = \pi D_1 N / (12)(60)$ and $D_1 = 360C(2gH)^{\frac{1}{2}} \cos \alpha_1 / \pi N$ To find the breadth of the wheel (L), where $s_0 = kD_1$, Equations (26), (27) and (28) may be used.

$$Q = \left(\frac{C s_0 L}{144} \right) (2gH)^{\frac{1}{2}} \tag{7}$$

$$L = 144 Q N / 862 H^{\frac{1}{2}} C k (2gH)^{\frac{1}{2}} \tag{8}$$

where $k = 0.075$ and 0.10 , respectively.

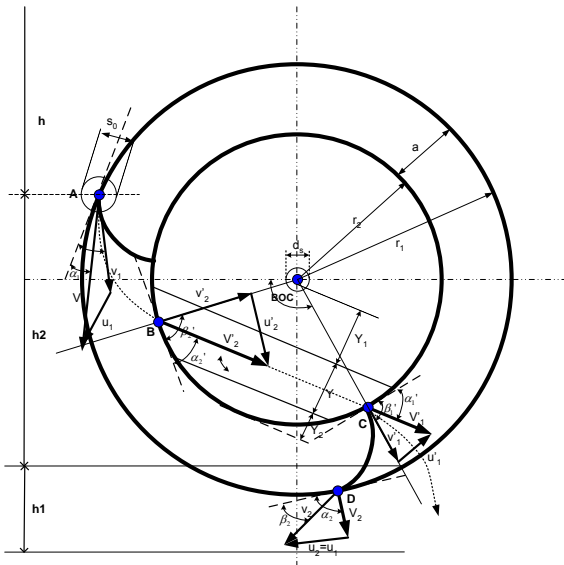


Fig. 6. Path of jet inside wheel [11]

2.2.4 Curvature of the blade

The curvature of the blade, as shown in Figure 7, is calculated using Equation (9)

$$\rho = \frac{[(r_1)^2 - (r_2)^2]}{2r_1 \cos \beta_1} \tag{9}$$

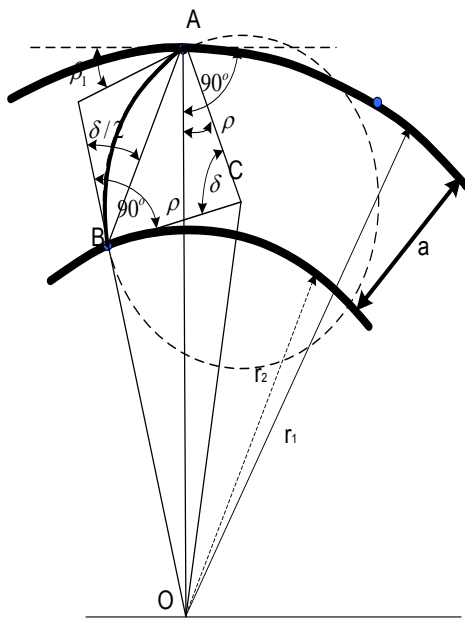


Fig. 7. Curvature of the blades [11]

2.2.5 Central Angle

The central angle, as shown in Figure 7, can be calculated using Equation (10).

$$\tan \frac{1}{2} \delta = \cos \beta_1 / (\sin \beta_1 + \frac{r_2}{r_1}) \tag{10}$$

In accordance with the construction design equations given above, our calculation results are shown in Table 1, using alpha angles of 15°, 16°, and 17°.

Table 1. Calculation results using the construction design

Blade Angle		Radial Rim Width			
α_1	β_1	r_2	a	α_2	bOC
15°	28°	0.64 r_1	0.18 D_1	52°	104°
16°	30°	0.66 r_1	0.17 D_1	53°	106°
17°	31°	0.668 r_1	0.165 D_1	53°	106°
Blade Angle		Wheel Diameter and Axial Wheel Breadth			
α_1	β_1	D_1	L		
15°	28°	$(870/N)H^{0.5}$	0.281QN /H until 0.21QN/H		
16°	30°	$(866/N)H^{0.5}$	0.282QN /H until 0.211QN/H		
17°	31°	$(862/N)H^{0.5}$	0.283QN /H until 0.212QN/H		
Blade Angle		Curvature of Blade	Central Angle		
α_1	β_1	ρ	δ		
15°	28°	0.334 r_1	77°		
16°	30°	0.326 r_1	74°		
17°	31°	0.323 r_1	72°		

2.3 Particle Swarm Optimization (PSO) Algorithm

American psychologist Kennedy and electrical engineer Eberhart developed the PSO algorithm based on the behavior of individuals in a swarm of birds [14]. The PSO algorithm is an optimization technique and also a kind of evolutionary computation technique. PSO is initialized to a random solution, using an iterative search for the optimal value[15]. Each individual in the group is called a particle in a D-dimension solution space. The position vector of the i_{th} particle is represented as $X_i=(X_{i1}, X_{i2}, \dots, X_{in})$. The best position found by the i_{th} particle so far is denoted as $P_i=(p_{i1}, p_{i2}, \dots, p_{in})$, and is known as p_{Best} ; Accordingly, the best position found by the whole swarm is denoted as $P_g=(P_{g1}, P_{g2}, \dots, P_{gn})$, and is known as G_{best} . The velocity vector of the i_{th} particle is represented as $V_i=(V_{i1}, V_{i2}, \dots, V_{in})$. The velocity and position of the i_{th} particle can be defined according to the following equations:

$$V_{in} = wV_m + c_1r_1(P_{in}-X_i) + c_2r_2(P_{gn}-X_{in}) \tag{10}$$

$$X_{in} = X_{in} + V_{in} \tag{11}$$

where w is a constriction factor, c_1 and c_2 are learning factors, and r_1 and r_2 are random numbers generated uniformly in the range [0-1].

A linearly decreasing inertia weight was first introduced by Shi and Eberhart in [14]. The linearly decreasing inertia weight is modified as

$$w(ite\text{r}) = w_{max} - \left(\frac{w_{max} - w_{min}}{ite\text{r}_{max}} \right) ite\text{r} \tag{12}$$

where w_{max} is the initial inertia weight, w_{min} is the final inertia weight, $ite\text{r}_{max}$ is the iteration maximum in the evolution process, and $ite\text{r}$ is the current value of the iteration. Normally, w_{max} is set to 0.9 and w_{min} is set to 0.4.

The following gives the design step for the improved version of the PSO algorithm [15],[16]

3. Problem Formulation

3.1 Optimization Formula

The input power and output power equations of the Banki turbine are affected by the value of the parameters H, g, C, ω, ψ, α₁, β₁, and β₂. Constant parameters, such as H, C, and g do not change their values when optimization is performed. The values we can optimize are the values of α₁, β₁, and β₂ with the goal of changing the angle of the corner to affect the efficiency of the turbine. The equation to optimize these parameters is as follows, by maximizing the overall value of equations (3), (1), (4), (2) The values of influence are the equality constraints:

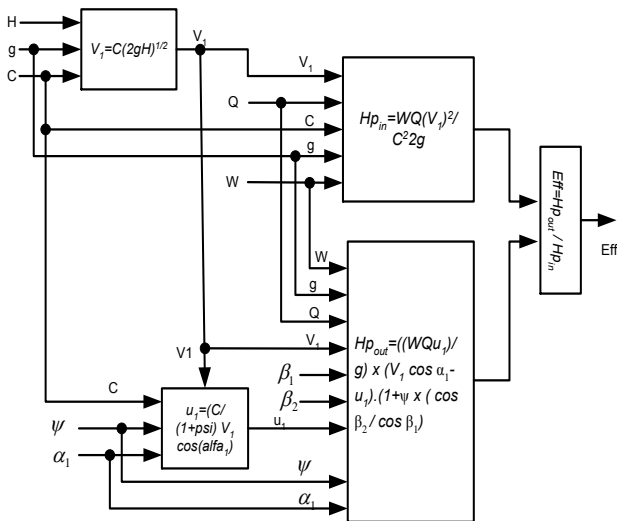


Fig. 8. Proposed Optimization Strategy

The inequality constraints are

$$\begin{aligned} \cos \alpha_1^{\min} &\leq \cos \alpha_1 \leq \cos \alpha_1^{\max} \\ \cos \beta_1^{\min} &\leq \cos \beta_1 \leq \cos \beta_1^{\max} \\ \cos \beta_2^{\min} &\leq \cos \beta_2 \leq \cos \beta_2^{\max}. \end{aligned}$$

3.2 Proposed Method Optimization

According to the block diagram of Figure 8 above, the value of V₁ will be influenced by the parameters H, g, and C. Furthermore, the value of V₁ is the input for U₁, H_{p_{in}}, and H_{p_{out}}. The value of U₁ will be determined by the values of the parameters C, ψ, α₁, and V₁. The H_{p_{in}} value is determined by the values of Q, C, g, ω, and V₁. The H_{p_{out}} value will be determined by the values of Q, V₁, g, ω, u₁, ψ, α₁, β₁, and β₂. The results of a comparison of the H_{p_{in}} and H_{p_{out}} values determine the value of the efficiency. We used MATLAB simulation in the optimization process to obtain the maximum value of the efficiency (η) by the value optimized angles α₁, β₁, and β₂.

4. Simulation Result

By the method proposed above in section 3.2, Equation (8) is optimized by MATLAB simulation. The initialization of the parameter values in the PSO algorithm includes the number of birds n = 50, dimensions = 3, steps = 50, c₂ = 0.3, c₁ = 0.1, w = 0.75 momentum, the angle of α₁ (15 ≤ α₁ ≤ 17), the angle of β₁ (28 ≤ β₁ ≤ 31), and the angle of β₂ (29 ≤ β₂ ≤ 32). The optimization results of Equation (8) are provided in Table 2.

First, PSO simulations were performed with the input values of H and Q, then the PSO calculates the values of α₁, β₁, β₂, V₁, H_{p_{in}}, U₁, H_{p_{out}}, and η. The range of H values is 1 ≤ H ≤ 60 and the Q value is either 30, 35, or 40. Every pair of values of H and Q is given 180 combinations, and for each combination of H and Q, the PSO will produce 30 lines of data. The next step is to identify combinations of H and Q with the highest efficiency (η). Of the 180 combinations, Table 2 shows that only 5 of these were chosen as having the highest η in the PSO simulation results.

Please note that the simulated data generated by the PSO values for 17° and 16° angles never appeared. On the basis of these findings, we had to conduct experiments (section 5) to validate the PSO results and prove that the 15° α₁ angle is better than 16° and 17° angles.

Table 2. Simulation results of the PSO algorithm

Data	1,0	2,0	3,0	4,0	5,0
H	56,0	47,0	26,0	27,0	58,0
Q	35,0	30,0	35,0	40,0	30,0
α ₁	15,0004	15,0004	15,0004	15,0002	15,0008
β ₁	28,1936	29,8677	29,8677	28,8056	29,2837
β ₂	31,6861	31,8705	31,8705	29,2072	30,0975
V ₁	10,3713	9,5015	7,0669	12,4734	14,9269
H _{p_{in}}	1960000,0	1410000,0	910000,0	1080000,0	1740000,0
u ₁	5,0	4,5	3,4	6,0	7,1
H _{p_{out}}	1738531,6	1250676,3	807173,2	957961,8	1543379,2
η	0,887006	0,887004	0,887004	0,887002	0,887000

5. Experimental Results

We constructed prototype turbine models with axles placed on two pillows so the turbine could spin with little friction, as shown in the photographs in Figure 11.

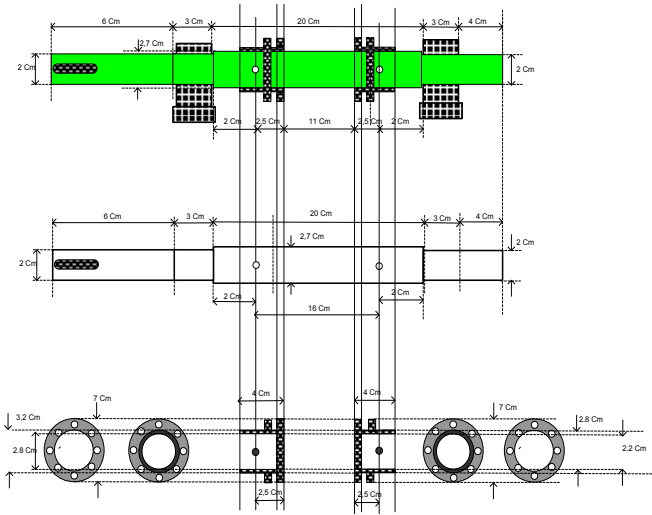


Fig. 9. Design shaft of the new micro turbine

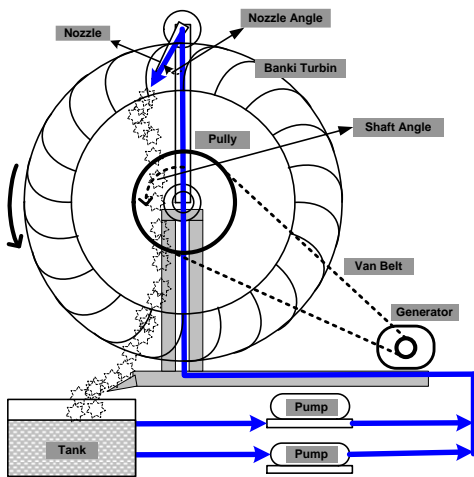


Fig. 10. Design model simulation of the micro turbine

The prototype models were each made of a waterwheel supported by two pillows placed on the left and right sides of a holder perpendicular to the shafts, with axles made of iron, a pulley as the fan belt connected to the generator, and a water pump to circulate the air from the tank to the nozzle. In this study we used as many as 16 blades with 50 cm wheel diameters and wheels 12 cm thick. The curvature of the waterwheel's blade angle is the factor responsible for generating a maximum efficiency value (η).



Fig. 11. Model of the turbine prototype

The angle value of $\alpha_1 = 15^\circ$, obtained from the simulation results in section 4, was tested, as were angles $\alpha_1 = 16^\circ$ and 17° .

To generate the water flow, we installed 2 pumps (Shimizu, Model PS-116 BIT, U: 1 x 220V 50Hz with $Q = 10\text{--}24$ l/min). Power input was calculated as $P_{in} = Q \times \rho \times g \times h$, where P_{in} = power input (watts), Q = volumetric water flow rate (m^3/s) = 0.00064, ρ = density of water (kg/m^3) = 1000, g = acceleration due to gravity ($= 9.81 \text{ m}/\text{s}^2$), and h = total energy difference between the upstream and downstream line of wheel (m) = 50 cm = 0.5 m. so, $P_{in} = 1000 \text{ kg}/\text{m}^3 \times 9.81 \text{ m}/\text{s}^2 \times 0.00064 \text{ m}^3/\text{s} \times 0.5 \text{ m} = 3.14 \text{ W}$, as the power input value for the efficiency value results.

Each turbine model was tested with curvature angles of $\alpha = 15^\circ, 16^\circ$, and 17° . The values of the other parameters were kept exactly the same in all models. Using a water pump to generate water flow to the nozzle, we changed the angle of the nozzle and measured the current I (amperes), voltage V (volts), and rpm. The power generated was calculated from $P = I \times V$ (watts).

An output efficiency graph can be drawn for the angle (θ) within the range $0^\circ\text{--}50^\circ$. Figure 12 shows a comparison of the efficiency output for blade angle curvatures (α) of $15^\circ, 16^\circ$, and 17° , respectively. The parameters of a water flow velocity of $0.00064 \text{ m}^3/\text{s}$, a 50 cm diameter water wheel, 16 blades, and a 12 cm-wide water wheel were the same in all models. The goal was to carefully investigate the effect of the curvature blade angle (α) on water wheel efficiency. Experiments were performed sequentially for each wheel at a certain curvature angle α to determine their influence. The value of the curvature of the blade angles (α) selected for testing was based on the results of the PSO (section 3). The best angle (α) according to our PSO is 15° . According to the results of the plans [12], 16° was the optimum, and 17° was the authors optimal experimental result by their own research. Our experimental results verified our results that a water wheel with a blade curvature angle (α) of 15° produces the highest nozzle angle (θ°) efficiency in the range $25^\circ < \theta^\circ < 45^\circ$, compared with water wheel angle curvatures of 16° and 17° .

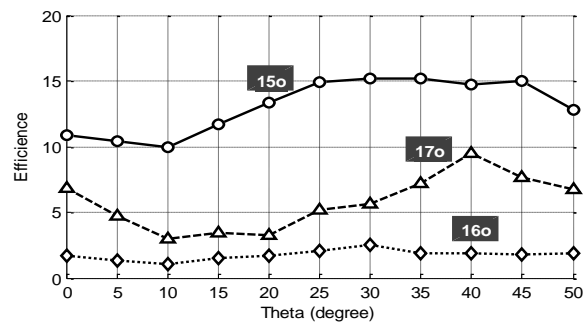


Fig. 12. Efficiency of the relative water wheel nozzle angle θ

Figure 13 shows the power output produced by the water wheel with a 15° blade curvature angle, which is higher than the output by water wheels with the blade curvature angles of 16° or 17° . The chart patterns formed by the power output are similar to the efficiency pattern. This is because efficiency is the ratio of the output power to the input power. In this case, the input power is constant.

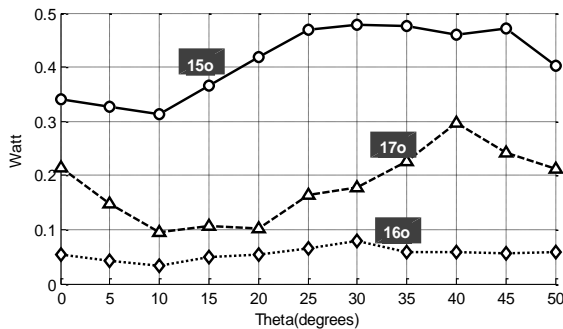


Fig. 13. Power output of the water wheel vs nozzle angle θ

The RPM output can be ascribed to the nozzle angle θ . In Figure 14 we can see that the RPM output value increases with an increasing nozzle angle from 10 $^\circ$ to 30 $^\circ$. These results show that a 15 $^\circ$ blade curvature angle (α) yields a higher RPM than the water wheels with 16 $^\circ$ and 17 $^\circ$ blade curvature angles (α). Other parameters were held constant in the three experiments.

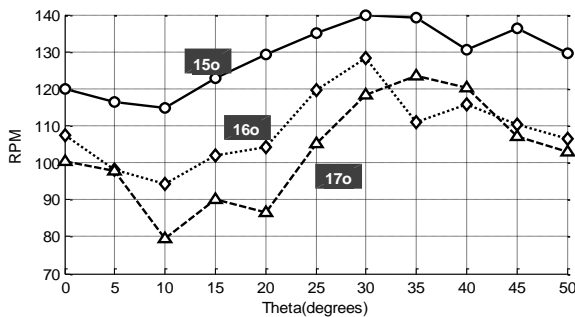


Fig. 14. RPM of the water wheel vs the nozzle angle θ

The improved results obtained with a 15 $^\circ$ blade curvature angle α compared with 16 $^\circ$ and 17 $^\circ$ blade curvature angles α include (1) RPM value, (2) output power, (3) output current, and (4) voltage output. We can conclude that water wheels with a 15 $^\circ$ blade curvature angle have higher efficiency compared with those with 16 $^\circ$ and 17 $^\circ$ blade curvature angles. Thus this study contradicts the research results of [12], which concluded that a 16 $^\circ$ blade curvature angle was optimal.

6. Conclusion

The angle of the blade greatly affects water wheel efficiency where the blade is in direct contact, such that the thrust of water causes the wheel to spin. A 15 $^\circ$ blade curvature angle is shown to produce higher efficiency values when compared with curvature angles of 16 $^\circ$ [12] and 17 $^\circ$. By utilizing the PSO algorithm to find the optimal blade curvature angle, the water wheel is proven to generate higher output power and higher RPM with its nozzle set at this angle (θ) value.

The energy generated by the water wheel with a 15 $^\circ$ blade curvature angle proved to be higher than those with curvature angles of 16 $^\circ$ [12] and 17 $^\circ$. These results were obtained from a mini-generator operating with a water wheel-mounted fixed load, for which the output current and voltage were measured. The output power of each model

were calculated, and the calculation results provide the evidence that the 15 $^\circ$ blade curvature angle (α) produces the highest energy, when compared with angles of 16 $^\circ$ and 17 $^\circ$.

Acknowledgements

The authors wish to convey their gratitude to the Ministry of Ristekdikti, Indonesia, which providing financial research Hibah Bersaing via LPPM Udayana University 2015-2016 contract No. 311-19/UN14.2/PNL.01.03/2015.

References

- [1] T. H. Ching, T. Ibrahim, F. I. A. Aziz, and N. M. Nor, "Renewable energy from UTP water supply," in *2011 International Conference on Electrical, Control and Computer Engineering (INECCE)*, 2011, pp. 142–147.
- [2] I. Ushiyama, "Renewable energy strategy in Japan," *Renew. Energy*, vol. 16, no. 1–4, pp. 1174–1179, Jan. 1999.
- [3] S. Paudel, N. Linton, U. C. E. Zanke, and N. Saenger, "Experimental investigation on the effect of channel width on flexible rubber blade water wheel performance," *Renew. Energy*, vol. 52, pp. 1–7, Apr. 2013.
- [4] A. Zaman and T. Khan, "Design of a Water Wheel For a Low Head Micro Hydropower System," *Journal Basic Science And Technology*, vol. 1(3), pp. 1–6, 2012.
- [5] L. Jasa, P. Ardana, and I. N. Setiawan, "Usaha Mengatasi Krisis Energi Dengan Memanfaatkan Aliran Pangkang Sebagai Sumber Pembangkit Listrik Alternatif Bagi Masyarakat Dusun Gambuk –Pupuan-Tabanan," in *Proceeding Seminar Nasional Teknologi Industri XV*, ITS, Surabaya, 2011, pp. B0377–B0384.
- [6] L. Jasa, A. Priyadi, and M. H. Purnomo, "An Alternative Model of Overshot Waterwheel Based on a Tracking Nozzle Angle Technique for Hydropower Converter | Jasa | International Journal of Renewable Energy Research (IJRER)," *Ilhami Colak*, vol. 4, no. No. 4, pp. 1013–1019, Dec. 2014.
- [7] T. Sakurai, H. Funato, and S. Ogasawara, "Fundamental characteristics of test facility for micro hydroelectric power generation system," presented at the International Conference on Electrical Machines and Systems, 2009. ICEMS 2009, 2009, pp. 1–6.
- [8] G. Muller, *Water Wheels as a Power Source*. 1899.
- [9] L. A. HAIMERL, "The Cross-Flow Turbine."
- [10] I. Vojtko, V. Fecova, M. Kocisko, and J. Novak-Marcincin, "Proposal of construction and analysis of turbine blades," in *2012 4th IEEE International Symposium on Logistics and Industrial Informatics (LINDI)*, 2012, pp. 75–80.
- [11] L. Jasa, A. Priyadi, and M. H. Purnomo, "Designing angle bowl of turbine for Micro-hydro at tropical area," in *2012 International Conference on Condition Monitoring and Diagnosis (CMD)*, Sept., pp. 882–885.
- [12] C. A. Mockmore and F. Merryfield, "The Banki Water Turbine," *Bull. Ser. No25*, Feb. 1949.
- [13] M. Geethanjali, S. M. Raja Slochanal, and R. Bhavani, "PSO trained ANN-based differential protection scheme

- for power transformers,” *Neurocomputing*, vol. 71, no. 4–6, pp. 904–918, Jan. 2008.
- [14] W. Dongsheng, Y. Qing, and W. Dazhi, “A novel PSO-PID controller application to bar rolling process,” in *Control Conference (CCC), 2011 30th Chinese*, 2011, pp. 2036–2039.
- [15] W. Cai, L. Jia, Y. Zhang, and N. Ni, “Design and Simulation of Intelligent PID Controller Based on Particle Swarm Optimization,” in *2010 International Conference on E-Product E-Service and E-Entertainment (ICEEE)*, 2010, pp. 1–4.
- [16] L. Jasa, Ika Putri, A. Priyadi, and M. H. Purnomo, “Design Optimization of Micro Hydro Turbin Using Artificial Particel Swarm Optimization and Artificial Neural Network,” *Kursor*, vol. 7, no. 3, pp. 135–144, oktober 2014.